
ELSEVIER Applied Mathematics and Computation 118 (2001) 223–246

APPLIED MATHEMATICS AND COMPUTATION

www.elsevier.com/locate/amc

Numerical experiments for advection–diffusion problems in a channel with a 180° bend

C. Clavero [a,*], J.J.H. Miller [b], E. O'Riordan [c], G.I. Shishkin [d]

[a] *Departamento de Matematica Aplicada, Universidad de Zaragoza, 50015 Zaragoza, Zaragoza, Spain*

[b] *Mathematics Department, Trinity College, Dublin 2, Ireland*

[c] *School of Mathematical Sciences, Dublin City University, Dublin 9, Ireland*

[d] *Institute of Mathematics and Mechanics, Ekaterinburg, Russia*

Abstract

In this paper we solve numerically two singularly perturbed linear convection–diffusion problems for heat transfer in a fluid with an assumed flow field in the neighbourhood of a 180° bend in a channel. In the first problem the theoretical solution has a parabolic boundary layer and in the second problem there is both a parabolic and a regular boundary layer in the solution. The numerical method uses piecewise uniform fitted meshes condensing in a neighbourhood of each boundary layer and a standard upwind finite difference operator satisfying a discrete maximum principle. The numerical results confirm computationally that the method is ε-uniform in the sense that the rate of convergence and the error constant of the method are independent of the singular perturbation parameter ε, where ε denotes the reciprocal of the Péclet number of the fluid. This ε-uniform behaviour is obtained only when an appropriate piecewise uniform fitted mesh is constructed for each boundary layer. This is confirmed by several additional computations on meshes which do not fulfill this requirement.

Keywords: Uniform convergence; Shishkin meshes; Parabolic and regular layer

* Corresponding author.

E-mail addresses: clavero@posta.unizar.es (C. Clavero), jmiller@tcd.ie (J.J.H. Miller), oriordae@ccmail.dcu.ie (E. O'Riordan), sgi@eqmph.imm.intec.ru (G.I. Shishkin).

0096-3003/01/$ - see front matter
PII: S0096-3003(99)00215-5

1. Introduction

Singularly perturbed differential equations are characterized by the presence of a small parameter ε multiplying the highest order derivatives. Such problems arise in many areas of applied mathematics. The solutions of singularly perturbed differential equations typically have steep gradients, in thin regions of the domain, whose magnitude depends inversely on some positive power of ε. Such regions are called either interior or boundary layers, depending on whether their location is in the interior or at the boundary of the domain.

The location and width of these layers depend on the local asymptotic nature of the solution of the differential equation. Layers described by an ordinary, parabolic or elliptic differential equation are called, respectively, regular, parabolic or elliptic layers. Numerical methods for which the error bounds are independent of the singular perturbation parameter ε are called ε-*uniform* methods.

In this paper, numerical results are presented for two singularly perturbed linear convection–diffusion problems for heat transfer in a fluid with an assumed flow field in the neighbourhood of a 180° bend in a channel. The singular perturbation parameter ε is the reciprocal of the Péclet number of the fluid. A key advantage of ε-uniform methods for practical problems is that the same numerical method is applicable whatever the material in the channel. In the first problem a parabolic layer appears in the solution. The second problem is more difficult because it has a parabolic layer on one part of the boundary and a regular layer on another part. The numerical results confirm computationally that these numerical methods, which use a standard upwind finite difference operator satisfying a maximum principle on a piecewise-uniform fitted mesh, are ε-uniform. That is, the pointwise error of the numerical solutions is guaranteed to decrease at a fixed rate as the mesh is refined regardless of the value of the Péclet number. In fact it has been established theoretically in [1] that such numerical methods are ε-uniform for a wide class of singularly perturbed problems, including the problems considered here.

Piecewise-uniform fitted meshes were first introduced and analyzed by Shishkin [2]. The first computations using such methods were presented in [3]. In [4] numerical results are presented for a simpler problem which has a parabolic, but no regular, layer. An introduction to the theory of fitted mesh methods is contained in [5].

It is important to note that we use the maximum norm in the entire domain to measure the pointwise error. Since piecewise uniform fitted meshes have points in the boundary layers it follows that the results we obtain are accurate not only outside, but also within the boundary layers. Furthermore, the pointwise errors within the boundary layers are found to be comparable in magnitude to those in the rest of the domain. This is in marked contrast to

previous results for problems of this type, where qualitative rather quantitative measures of the accuracy are employed.

2. Statement of the problem

Letting θ denote the temperature, $\vec{u} = (u_1, u_2)$ the velocity of the fluid and $\varepsilon = 1/Pe$, (where Pe is the Péclet number) the coefficient of diffusion, the transfer of heat in a two-dimensional region Ω is described by the following linear convection–diffusion equation:

$$\nabla \cdot (-\varepsilon \nabla \theta + \vec{u}\theta) = f \quad \text{in } \Omega, \tag{2.1a}$$

where it is assumed that Ω is a bounded domain with Lipschitz continuous boundary Γ. Let Γ_D and Γ_N, respectively denote the parts of Γ on which Dirichlet and Neumann boundary conditions are specified, where $\Gamma = \Gamma_D \cup \Gamma_N$ and $\Gamma_D \cap \Gamma_N = \emptyset$. Let $\vec{n}$ denote the outward unit normal on Γ. The inflow and outflow boundaries Γ_i and Γ_o are defined, respectively by

$$\Gamma_o = \{(x,y) \in \Gamma : (\vec{u} \cdot \vec{n})(x,y) > 0\},$$
$$\Gamma_i = \{(x,y) \in \Gamma : (\vec{u} \cdot \vec{n})(x,y) < 0\}.$$

It is assumed that $\Gamma_D \supset \Gamma_i$, that the diffusion coefficient ε is positive and that $\nabla \cdot \vec{u} = 0$. The latter condition means that the flow is incompressible. When $\varepsilon \ll 1$, the differential Eq. (2.1a) is singularly perturbed and the flow is said to be convection dominated.

In the convection dominated case, the solution of this linear problem can exhibit various singularities, depending on the choice of boundary conditions, and it can be decomposed into the sum of a smooth and a singular component for each kind of singularity. In this paper we consider problems exhibiting two different types of singularities. In Problem 1 we choose boundary conditions so that there is just one kind of singularity, namely a parabolic boundary layer, and in the second problem we take the boundary conditions so that the solution has a parabolic layer at one part of the boundary and a regular layer at another. The main goal of this paper is to construct appropriate fitted mesh methods to obtain ε-uniformly accurate solutions for both of these particular problems. Because of the linearity, it is clear that similar numerical methods will give ε-uniformly accurate solutions of any general linear problem having these types of singularities.

In both problems Dirichlet and Neumann boundary conditions of the following form are used:

$$\theta = g \quad \text{on } \Gamma_D, \tag{2.1b}$$

$$\frac{\partial \theta}{\partial n} = 0 \quad \text{on } \Gamma_N. \tag{2.1c}$$

The streamlines of the reduced equation corresponding to (2.1a) are in the direction $\vec{u}$. The boundary is said to be characteristic at a point $(x,y) \in \Gamma$ if the tangent to Γ at that point is in the direction $\vec{u}$. Equivalently, Γ is characteristic at each point $(x,y) \in \Gamma$ at which

$$(\vec{u} \cdot \vec{n})(x,y) = 0.$$

In what follows the domain is $\Omega = (-1,1) \times (0,1)$ and the flow field $\vec{u}$ is taken to be [6]

$$\vec{u}(x,y) = (2y(1-x^2), -2x(1-y^2))^{\mathrm{T}}. \tag{2.1d}$$

Thus the components of $\vec{u}$ vanish and change sign at various points of $\overline{\Omega}$. The inhomogenous term f is assumed to satisfy

$$f(x,y) \equiv 0. \tag{2.1e}$$

It follows from the definitions that $\Gamma_{\mathrm{i}} = \{(x,0): -1 < x < 0\}$ and $\Gamma_{\mathrm{o}} = \{(x,0): 0 < x < 1\}$. This corresponds to heat transfer in a fluid with the assumed flow field in the neighbourhood of a 180° bend of the channel.

In Problem 1 the Neumann part Γ_{N} of the boundary is taken to be

$$\Gamma_{\mathrm{N}} = \Gamma_{\mathrm{o}}. \tag{2.1f}$$

On the Dirichlet part Γ_{D} of the boundary the boundary conditions are defined by

$$g(x,y) = \begin{cases} 1-y & \text{on } \Gamma_e, \\ \sin^4(x+\frac{1}{2}) & \text{on } \Gamma_f, \\ 0 & \text{on } \Gamma_{\mathrm{D}} \setminus \Gamma_e \cup \Gamma_f), \end{cases} \tag{2.1g}$$

where $\Gamma_e = \{(1,y): 0 < y < 1\}$ and $\Gamma_f = \{(x,0): -1/2 \leqslant x \leqslant 0\}$. This choice of boundary conditions ensures compatibility and that the only boundary layer in the solution is a parabolic layer in a neighbourhood of the edge Γ_e.

In [7] Hutton considered a similar problem with the Dirichlet boundary conditions

$$g(x,y) = \begin{cases} 1 + \tanh(20x+10) & \text{on } \Gamma_{\mathrm{i}}, \\ 0 & \text{on } \Gamma_{\mathrm{D}} \setminus \Gamma_{\mathrm{i}}. \end{cases}$$

With this choice the solution has no boundary layers. His problem demonstrates the effects of cross-stream diffusion when the streamlines are not parallel to the co-ordinate axes. A further study of the problem was made in [8] with the Dirichlet boundary conditions

$$g(x,y) = \begin{cases} 1 + \tanh(20x+10) & \text{on } \Gamma_{\mathrm{i}}, \\ 100 & \text{on } \Gamma_e, \\ 0 & \text{on } \Gamma_{\mathrm{D}} \setminus (\Gamma_{\mathrm{i}} \cup \Gamma_e). \end{cases}$$

The solution of this problem exhibits a parabolic boundary layer in a neighbourhood of the edge Γ_e, but it also has an additional discontinuity arising from an incompatibility of the boundary conditions at the corner point (1,1). Our choice of Dirichlet boundary conditions (2.1g) is more suitable for the investigation of the effect of a parabolic boundary layer, because it is not complicated by any further effect due to an incompatibility in the boundary conditions, as is the case with Scotney's choice. Numerical experiments using higher-order finite difference schemes on problems similar to those considered by Hutton and Scotney were reported in [9,6]. A recent comprehensive discussion of such problems and their numerical solution is contained in [10]. In [4] Clavero et al. applied a similar numerical method to that used in the present paper for the following choice of Dirichlet boundary conditions

$$g(x,y) = \begin{cases} 1-y & \text{on } \Gamma_e, \\ 0 & \text{on } \Gamma_D \setminus \Gamma_e, \end{cases}$$

and thus $g = 0$ on the inflow boundary Γ_i. At the end of the present paper, we show computationally that non-zero boundary conditions on Γ_i do not influence the uniform convergence of this numerical method.

In Problem 2, $\Gamma_D = \partial\Omega$ and the boundary conditions are given by (see Fig. 1)

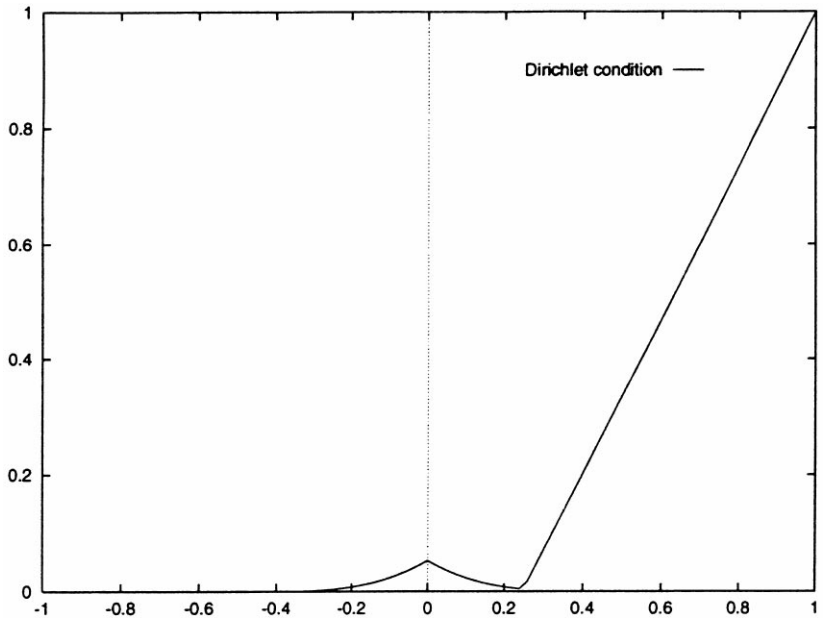

Fig. 1. Sketch of the boundary value $\theta(x,0)$ for Problem 2.

$$g(x,y)=\begin{cases}1-y & \text{on } \Gamma_e,\\ \sin^4(x+1/2) & \text{on } \Gamma_f,\\ \sin^4(-x+1/2) & \text{on } \Gamma_g,\\ 4[x-1/4-(x-1)\sin^4(1/4)]/3 & \text{on } \Gamma_h,\\ 0 & \text{on } \Gamma_{\mathrm{D}}\setminus(\Gamma_e\cup\Gamma_f\cup\Gamma_g\cup\Gamma_h),\end{cases} \tag{2.1h}$$

where $\Gamma_e=\{(1,y)\colon 0<y<1\}$, $\Gamma_f=\{(x,0)\colon -1/2\leqslant x\leqslant 0\}$, $\Gamma_g=\{(x,0)\colon 0\leqslant x\leqslant 1/4\}$, $\Gamma_h=\{(x,0)\colon 1/4\leqslant x\leqslant 1\}$.

This choice of boundary conditions ensures compatibility at the corners of Ω and that we have two types of singularity in the solution, namely a parabolic layer in a neighbourhood of the edge Γ_e and a regular layer in a neighbourhood of the boundary Γ_h. Note that the boundary conditions are symmetric on Γ_f and Γ_g, and so the regular layer occurs only on Γ_h. Without this symmetry the problem is more complicated and the numerical method used here is not suitable.

Both uniform and piecewise-uniform meshes are used to discretize the domain Ω. Since the piecewise uniform meshes are problem-dependent, their construction is described later for each problem separately. Mesh functions defined on the mesh $\Omega^{N\times N}$ are denoted by θ^N, and the following mesh parameters are introduced:

$$\begin{aligned} &h_i=x_i-x_{i-1}, \quad \tilde{h}_{i+1}=(h_{i+1}+h_i)/2,\\ &k_j=y_j-y_{j-1}, \quad \tilde{k}_{j+1}=(k_{j+1}+k_j)/2.\end{aligned} \tag{2.2}$$

We write $\theta_{i,j}=\theta^N(x_i,y_j)$. On $\Omega^{N\times N}$ the following upwind finite difference operator is defined by

$$\begin{aligned} &-\varepsilon(\delta_x^2+\delta_y^2)\theta^N+\tilde{D}_x(u_1\theta^N)+\tilde{D}_y(u_2\theta^N)=0\\ &\quad \text{for } i=1,\ldots,N-1;\ \ j=1,\ldots,N-1;\end{aligned} \tag{2.3a}$$

where $\tilde{D}_x$ is the first order upwind finite difference operator

$$\tilde{D}_x(u_1\theta^N)\equiv\frac{u_{1;i,j}-|\,u_{1;i,j}\,|}{2}D_x^+\theta_{i,j}+\frac{u_{1;i,j}+|\,u_{1;i,j}\,|}{2}D_x^-\theta_{i,j}, \tag{2.3b}$$

$$D_x^-\theta_{i,j}\equiv\frac{\theta_{i,j}-\theta_{i-1,j}}{h_i} \quad \text{and} \quad D_x^+\theta_{i,j}\equiv\frac{\theta_{i+1,j}-\theta_{i,j}}{h_{i+1}}. \tag{2.3c}$$

The operator $\tilde{D}_y$ is defined analogously. The standard second order centered finite difference is

$$\delta_x^2\theta_{i,j}\equiv\frac{D_x^+\theta_{i,j}-D_x^-\theta_{i,j}}{\tilde{h}_{i+1}}, \tag{2.3d}$$

and δ_y^2 is defined analogously. The boundary conditions are discretized as follows:

Problem 1.

$$\frac{\theta_{i,1}-\theta_{i,0}}{k_1}=0 \quad \text{for } i=\frac{N}{2}+1,\ldots,N-1, \tag{2.3e}$$

$$\theta_{i,0}=0 \quad \text{for } i=0,\ldots,N_0, \text{ where } x_{N_0}<-c_1\leqslant x_{N_0+1}, \tag{2.3f}$$

$$\theta_{i,0}=h(x_i) \quad \text{for } i=N_0+1,\ldots,\frac{N}{2}, \tag{2.3g}$$

$$\theta_{i,M}=0 \quad \text{for } i=0,\ldots,N-1, \tag{2.3h}$$

$$\theta_{0,j}=0 \quad \text{for } j=1,\ldots,N-1, \tag{2.3i}$$

$$\theta_{N,j}=1-y_j \quad \text{for } j=0,\ldots,N. \tag{2.3j}$$

Problem 2.

$$\theta_{i,0}=0 \quad \text{for } i=0,\ldots,N_0, \text{ where } x_{N_0}<-c_1\leqslant x_{N_0+1}, \tag{2.3k}$$

$$\theta_{i,0}=h_1(x_i) \quad \text{for } i=N_0+1,\ldots,\frac{N}{2}, \tag{2.3l}$$

$$\theta_{i,0}=h_1(-x_i) \quad \text{for } i=\frac{N}{2}+1,\ldots,N_1 \text{ where } x_{N_1}<c_2\leqslant x_{N_1+1}, \tag{2.3m}$$

$$\theta_{i,0}=h_2(x_i) \quad \text{for } i=N_1+1,\ldots,N-1, \tag{2.3n}$$

$$\theta_{i,M}=0 \quad \text{for } i=0,\ldots,N-1, \tag{2.3o}$$

$$\theta_{0,j}=0 \quad \text{for } j=1,\ldots,N-1, \tag{2.3p}$$

$$\theta_{N,j}=1-y_j \quad \text{for } j=0,\ldots,N. \tag{2.3q}$$

Since the matrix associated with the numerical method (2.3a)–(2.3j) is an M-matrix, the upwind finite difference operator in (2.3a) satisfies a discrete maximum principle and the finite difference method (2.3a)–(2.3j) is stable. The same conclusions are valid for the finite difference method (2.3a)–(2.3d) and (2.3k)–(2.3q).

3. Numerical results on uniform meshes

Since the exact solutions of these problems are not known, the pointwise errors $\mid \theta^N(x_i,y_j)-\theta(x_i,y_j) \mid$ are approximated for successive values of ε on the six coarser meshes by $e_\varepsilon^N(i,j)=\mid \theta^N(x_i,y_j)-\theta^{512}(x_i,y_j) \mid$, where the superscript indicates the number of mesh elements used in the x-direction. That is, in the expression for the error the unknown exact solution is replaced by the approximate solution on the finest mesh. For each ε the maximum nodal error is approximated by

$$E_\varepsilon^N = \|e_\varepsilon^N\|_{\Omega^{N\times N}}, \tag{3.1}$$

where $\|w\|_{\Omega^{N\times N}} = \max_{(x_i,x_j)\in\Omega^{N\times N}} |w(x_i,y_j)|$ is the maximum norm on the mesh $\Omega^{N\times N}$, and for each N, the ε-uniform maximum nodal error is defined by

$$E^N = \max_\varepsilon E_\varepsilon^N. \tag{3.2}$$

The ε-uniform rate of convergence can be estimated using the double-mesh principle (see e.g. [11]). A numerical method for solving (2.1a)–(2.1g) is said to have an ε-uniform rate of convergence p on the sequence of meshes $\{\Omega^{N,N}\}_1^\infty$ if there exists an N_0, independent of ε, such that for all $N \geqslant N_0$

$$\sup_{0<\varepsilon\leqslant 1} \|\theta - \theta^N\|_{\Omega^{N\times N}} \leqslant CN^{-p},$$

where θ is the solution of (2.1a)–(2.1g), θ^N is the numerical approximation to θ, C and $p > 0$ are independent of ε and N.

In this paper an iterative method is used to solve the discretized equations. The relaxed incomplete LU-factorisation method [12] and the preconditioned conjugate gradient squared method are used, where the convergence criteria on the residuals is taken to be $\|r_k\| \leqslant 10^{-6}$.

In this section, problems (2.1a)–(2.1g) and (2.1a)–(2.1e) (2.1h) are solved using a numerical method composed of the upwind finite difference operator (2.3a)–(2.3q) on a sequence of uniform meshes $\Omega^{N\times N}$, with $N = 8, 16, 32, 64, 128, 256, 512$. Computed values of E_ε^N and E^N are given in Table 1 for Problem 1 and in Table 2 for Problem 2 for various values of ε and N.

Note that the maximum nodal error E^N does not decrease significantly as the mesh is refined. Such behaviour indicates computationally that this numerical method is not ε-uniform for both problems. It is important to note that the accuracy of the approximations E^N to the exact error decreases as we move to the right in the table, because the exact solution has been replaced by θ^{512}. More accurate values of the errors for this case are given in Table 7.

4. An ε-uniform numerical method for Problem 1

Piecewise-uniform fitted meshes $\Omega_\tau^{N\times N}$ for Problem 1 are constructed as follows. A one-dimensional piecewise uniform fitted mesh Ω_τ^N is constructed in the x-direction and a one-dimensional uniform mesh Ω^N in the y-direction. The mesh $\Omega_\tau^{N\times N}$ is then defined to be the tensor product $\Omega_\tau^N \times \Omega^N$ of these two one-dimensional meshes. The mesh Ω_τ^N is fitted for Problem 1 as follows. First, the interval $[-1,1]$ is subdivided into the three subintervals $[-1,0], [0,1-\tau]$, $[1-\tau,1]$ where the transition point τ is defined by

Table 1
Maximum nodal errors E_ε^N and E^N on uniform meshes for Problem 1

ε	N				
	8	16	32	64	128
2^0	4.899E − 2	2.893E − 2	1.482E − 2	7.021E − 3	3.018E − 3
2^{-2}	3.279E − 2	2.775E − 2	1.561E − 2	7.481E − 3	3.177E − 3
2^{-4}	**6.486E − 2**	3.300E − 2	1.797E − 2	8.765E − 3	3.857E − 3
2^{-6}	5.480E − 2	**6.474E − 2**	3.129E − 2	1.611E − 2	7.218E − 3
2^{-8}	1.627E − 2	5.284E − 2	**6.068E − 2**	2.770E − 2	1.323E − 2
2^{-10}	1.194E − 2	1.566E − 2	5.117E − 2	**5.523E − 2**	2.291E − 2
2^{-12}	1.401E − 2	1.440E − 2	1.545E − 2	4.877E − 2	**4.695E − 2**
2^{-14}	1.458E − 2	1.607E − 2	1.057E − 2	1.533E − 2	4.391E − 2
2^{-16}	1.472E − 2	1.652E − 2	1.153E − 2	6.407E − 3	1.506E − 2
2^{-18}	1.476E − 2	1.664E − 2	1.179E − 2	6.564E − 3	3.894E − 3
2^{-20}	1.477E − 2	1.667E − 2	1.186E − 2	6.699E − 3	3.449E − 3
2^{-22}	1.477E − 2	1.667E − 2	1.188E − 2	6.733E − 3	3.463E − 3
2^{-24}	1.477E − 2	1.668E − 2	1.188E − 2	6.742E − 3	3.466E − 3
2^{-26}	1.477E − 2	1.668E − 2	1.188E − 2	6.745E − 3	3.468E − 3
2^{-28}	1.477E − 2	1.668E − 2	1.188E − 2	6.745E − 3	3.468E − 3
2^{-30}	1.477E − 2	1.668E − 2	1.188E − 2	6.745E − 3	3.468E − 3
2^{-32}	1.477E − 2	1.668E − 2	1.188E − 2	6.745E − 3	3.468E − 3
E^N	0.0649	0.0647	0.0607	0.0552	0.0469

Table 2
Maximum nodal errors E_ε^N and E^N on uniform meshes for Problem 2

ε	N				
	8	16	32	64	128
2^0	1.792E − 2	1.019E − 2	5.306E − 3	2.647E − 3	1.230E − 3
2^{-2}	3.259E − 2	1.649E − 2	8.526E − 3	4.068E − 3	1.765E − 3
2^{-4}	**1.448E − 1**	1.019E − 1	5.743E − 2	3.071E − 2	1.403E − 2
2^{-6}	1.007E − 1	**1.417E − 1**	**1.474E − 1**	1.118E − 1	5.950E − 2
2^{-8}	2.956E − 2	7.947E − 2	1.054E − 1	**1.128E − 1**	**1.238E − 1**
2^{-10}	1.194E − 2	2.291E − 2	6.522E − 2	7.911E − 2	6.950E − 2
2^{-12}	1.401E − 2	1.440E − 2	1.919E − 2	5.597E − 2	5.929E − 2
2^{-14}	1.458E − 2	1.607E − 2	1.057E − 2	1.723E − 2	4.755E − 2
2^{-16}	1.472E − 2	1.652E − 2	1.153E − 2	6.300E − 3	1.602E − 2
2^{-18}	1.476E − 2	1.664E − 2	1.179E − 2	6.564E − 3	4.137E − 3
2^{-20}	1.477E − 2	1.667E − 2	1.186E − 2	6.699E − 3	3.433E − 3
2^{-22}	1.477E − 2	1.667E − 2	1.188E − 2	6.733E − 3	3.459E − 3
2^{-24}	1.477E − 2	1.668E − 2	1.188E − 2	6.743E − 3	3.465E − 3
2^{-26}	1.477E − 2	1.668E − 2	1.188E − 2	6.745E − 3	3.467E − 3
2^{-28}	1.477E − 2	1.668E − 2	1.188E − 2	6.745E − 3	3.467E − 3
2^{-30}	1.477E − 2	1.668E − 2	1.188E − 2	6.745E − 3	3.468E − 3
2^{-32}	1.477E − 2	1.668E − 2	1.188E − 2	6.745E − 3	3.468E − 3
E^N	0.1448	0.1417	0.1474	0.1128	0.1238

$$\tau = \min\left\{\frac{1}{2}, \sqrt{\varepsilon}\ln N\right\}. \tag{4.1}$$

Then, on each subinterval, a uniform mesh is constructed using $N/2$ mesh points in $[-1,0]$, and $N/4$ mesh points in both of the subintervals $[0,1-\tau]$ and $[1-\tau,1]$. The piecewise uniform fitted mesh on $\overline{\Omega}$ is then

$$\overline{\Omega}_{\tau}^{N\times N} = \{(x_i,y_j)\colon 0\leqslant i,j\leqslant N\}, \tag{4.2a}$$

where

$$x_i = \begin{cases} -1+\frac{2i}{N} & \text{for } 0\leqslant i\leqslant N/2, \\ \frac{4(1-\tau)(i-N/2)}{N} & \text{for } N/2 < i\leqslant 3N/4, \\ 1-\tau+\frac{4\tau(i-3N/4)}{N} & \text{for } 3N/4 < i\leqslant N \end{cases} \tag{4.2b}$$

and

$$y_j = j/N \quad \text{for } 0\leqslant j\leqslant N.$$

Note that $\Omega_{\tau}^{N\times N}$ is a uniform mesh on the domain Ω when ε or N are sufficiently large.

The problem (2.1a)–(2.1g), is now solved using a numerical method composed of the upwind difference operator (2.3a)–(2.3q) on the sequence of piecewise uniform fitted meshes $\Omega_{\tau}^{N\times N}$ with $N = 8, 16, 32, 64, 128, 256, 512$. The errors $|\,\theta^N(x_i,y_j) - \theta(x_i,y_j)\,|$ are approximated, for successive values of ε, on the six coarser meshes, by $e_{\varepsilon}^N(i,j) = |\,\theta^N(x_i,y_j) - \theta_I^{512}(x_i,y_j)\,|$, where the superscript N indicates the number of mesh elements used and the subscript I denotes bilinear interpolation. For each ε and N the maximum nodal error is approximated by

$$E_{\varepsilon}^N = \max_{i,j}\ e_{\varepsilon}^N(i,j), \tag{4.3}$$

and for each N the ε-uniform maximum nodal error is defined by

$$E^N = \max_{\varepsilon}\ E_{\varepsilon}^N. \tag{4.4}$$

Computed values of E_{ε}^N and E^N for problem (2.1a)–(2.1g) are given in Table 3 for various values of ε and N.

The numerical behaviour indicated by Table 3 is quite different qualitatively from that in Table 1. Note that, for each fixed value of ε, the errors E_{ε}^N decrease monotonically as the mesh is refined. Furthermore, the errors E^N decrease monotonically for increasing N and at a much faster rate than in Table 1. Indeed, for $N = 128$ the result is an order of magnitude better. Hence, increasing the computational effort yields greater accuracy, which is the intuitively correct behaviour for a numerical method to be considered satisfactory.

Table 3
Maximum nodal errors E_{ε}^{N} and E^{N} on piecewise uniform fitted meshes for Problem 1

ε	N				
	8	16	32	64	128
2^{0}	4.899E − 2	2.893E − 2	1.482E − 2	7.021E − 3	3.018E − 3
2^{-2}	3.279E − 2	2.775E − 2	1.561E − 2	7.481E − 3	3.177E − 3
2^{-4}	6.486E − 2	3.300E − 2	1.797E − 2	8.765E − 3	3.857E − 3
2^{-6}	**6.610E − 2**	**4.663E − 2**	**2.844E − 2**	**1.611E − 2**	7.218E − 3
2^{-8}	6.320E − 2	4.482E − 2	2.680E − 2	1.537E − 2	**7.483E − 3**
2^{-10}	6.172E − 2	4.452E − 2	2.663E − 2	1.532E − 2	7.470E − 3
2^{-12}	6.085E − 2	4.435E − 2	2.654E − 2	1.530E − 2	7.462E − 3
2^{-14}	6.039E − 2	4.427E − 2	2.650E − 2	1.529E − 2	7.457E − 3
2^{-16}	6.015E − 2	4.422E − 2	2.647E − 2	1.528E − 2	7.455E − 3
2^{-18}	6.003E − 2	4.420E − 2	2.646E − 2	1.528E − 2	7.454E − 3
2^{-20}	5.997E − 2	4.419E − 2	2.646E − 2	1.527E − 2	7.452E − 3
2^{-22}	5.994E − 2	4.418E − 2	2.645E − 2	1.527E − 2	7.452E − 3
2^{-24}	5.992E − 2	4.418E − 2	2.645E − 2	1.527E − 2	7.453E − 3
2^{-26}	5.991E − 2	4.418E − 2	2.645E − 2	1.527E − 2	7.458E − 3
2^{-28}	5.991E − 2	4.418E − 2	2.645E − 2	1.527E − 2	7.449E − 3
2^{-30}	5.990E − 2	4.418E − 2	2.645E − 2	1.527E − 2	7.449E − 3
2^{-32}	5.990E − 2	4.418E − 2	2.644E − 2	1.527E − 2	7.449E − 3
E^{N}	0.0661	0.0466	0.0284	0.0161	0.0075

The numerical solutions of Problem 1 for $\varepsilon = 2^{-10}$ on, respectively the uniform mesh and the fitted mesh $\Omega_{\tau_1,\tau_2}^{32\times 32}$ are shown in Figs. 2 and 3. Another view is obtained by comparing the contour plots of the numerical solution of Problem 1 for $\varepsilon = 2^{-10}$ on the uniform mesh $\Omega^{32\times 32}$ in Fig. 4, on the fitted mesh $\Omega_{\tau_1,\tau_2}^{32\times 32}$ in Fig. 5 and on the fitted mesh $\Omega_{\tau_1,\tau_2}^{256\times 256}$ in Fig. 6.

In Table 4 the computed rates of convergence p for Problem 1 using piecewise uniform fitted meshes are presented. These computed rates are consistent with the theoretical rates of ε-uniform convergence stated in the theorem in Appendix A. They suggest computationally that for Problem 1 the ε-uniform rate of convergence of this method is approaching $p = 1$.

5. An ε-uniform numerical method for Problem 2

In this section we want to solve the problem (2.1a)–(2.1e), (2.1h). This problem is more difficult than the previous one, because we have two different types of boundary layers. Each fitted mesh $\Omega_{\tau_1,\tau_2}^{N\times N}$ defined in what follows is the tensor product of two one-dimensional piecewise uniform fitted meshes, fitted in the x-direction for the parabolic layer and in the y-direction for the regular layer, and the numerical method is composed of the standard upwind finite

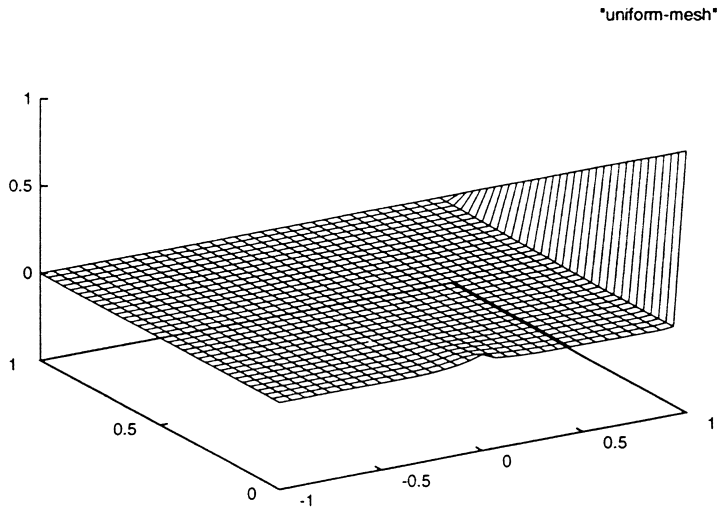

Fig. 2. Surface plot of the numerical solution of Problem 1 for $\varepsilon = 2^{-10}$ on the uniform mesh $\Omega^{32\times 32}$.

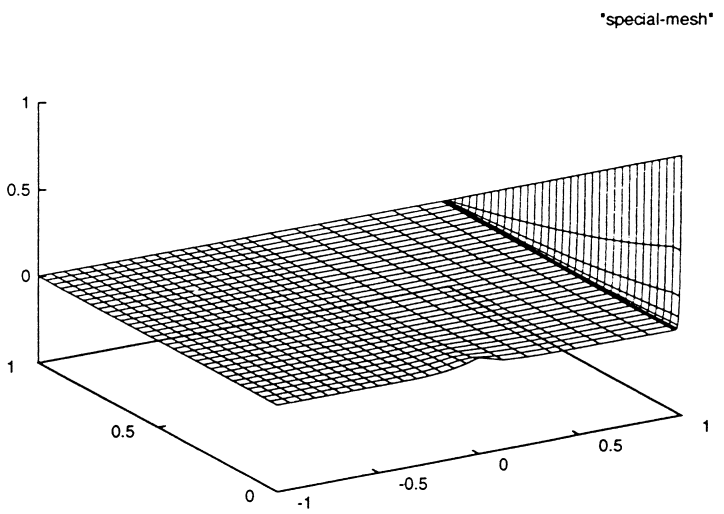

Fig. 3. Surface plot of the numerical solution of Problem 1 for $\varepsilon = 2^{-10}$ on the fitted mesh $\Omega^{32\times 32}_{\tau_1,\tau_2}$.

difference operator (2.3a)–(2.3q) on a sequence of these meshes with $N = 8, 16, 32, 64, 128, 256, 512$.

The piecewise-uniform fitted mesh in the x-direction is defined on the interval $[-1, 1]$ by subdividing it into the three subintervals $[-1, 0], [0, 1-\tau_1]$, $[1-\tau_1, 1]$ where the transition point

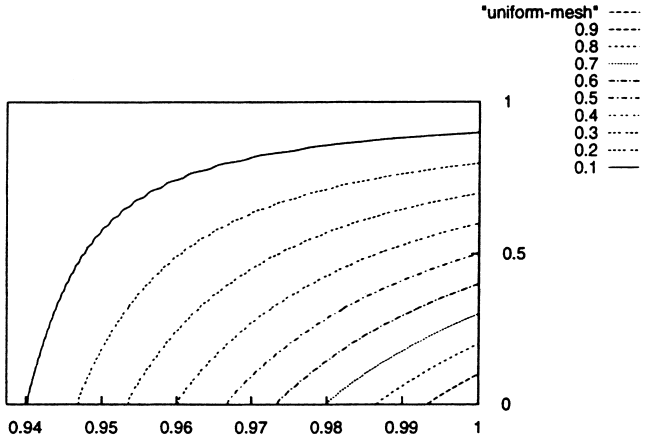

Fig. 4. Contour plot of the numerical solution of Problem 1 for $\varepsilon = 2^{-10}$ on the uniform mesh $\Omega^{32\times 32}$ in a neighbourhood of the edge $x = 1$.

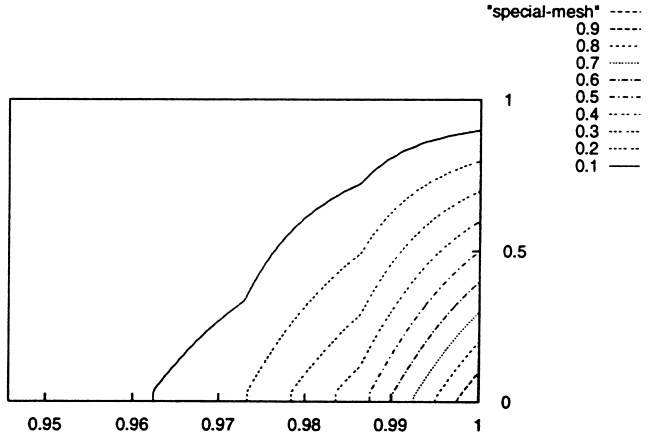

Fig. 5. Contour plot of the numerical solution of Problem 1 for $\varepsilon = 2^{-10}$ on the fitted mesh $\Omega^{32\times 32}_{\tau_1,\tau_2}$ in a neighbourhood of the edge $x = 1$.

$$\tau_1 = \min\left\{\frac{1}{2}, \sqrt{\varepsilon}\ln N\right\}. \tag{5.1}$$

The points of this piecewise uniform fitted mesh $\Omega^N_{\tau_1}$ in the x-direction are then defined by

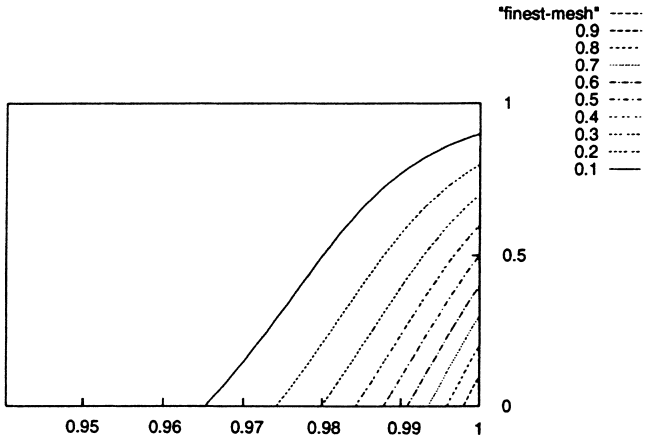

Fig. 6. Contour plot of the numerical solution of Problem 1 for $\varepsilon = 2^{-10}$ on the fine fitted mesh $\Omega^{256\times256}_{\tau_1,\tau_2}$ in a neighbourhood of the edge $x = 1$.

Table 4
Computed rates of convergence p on piecewise uniform fitted meshes $\Omega^{N\times N}_{\tau}$ for Problem 1

ε	N			
	8	16	32	64
2^{0}	0.759	0.964	1.078	1.217
2^{-2}	0.240	0.830	1.061	1.235
2^{-4}	0.975	0.877	1.036	1.184
2^{-6}	0.503	0.713	0.820	1.159
2^{-8}	0.496	0.742	0.802	1.039
2^{-10}	0.471	0.741	0.797	1.037
2^{-12}	0.456	0.741	0.795	1.036
2^{-14}	0.448	0.740	0.793	1.036
.	.	.	.	.
.	.	.	.	.
.	.	.	.	.
2^{-32}	0.439	0.740	0.792	1.036

$$x_i = \begin{cases} -1 + \frac{2i}{N} & \text{for } 0 \leqslant i \leqslant N/2, \\ \frac{4(1-\tau_1)(i-N/2)}{N} & \text{for } N/2 < i \leqslant 3N/4, \\ 1 - \tau_1 + \frac{4\tau_1(i-3N/4)}{N} & \text{for } 3N/4 < i \leqslant N. \end{cases} \tag{5.2}$$

The piecewise-uniform fitted mesh in the y-direction is defined on the interval $[0,1]$ by subdividing it into the two subintervals $[0,\tau_2],[\tau_2,1]$. Here the transition point τ_2 is defined by

$$\tau_2 = \min\left\{\frac{1}{2}, C\varepsilon \ln N\right\}, \tag{5.3}$$

where the constant C is taken to be

$$C = 2.1.$$

(Note that this value for C is used for the computations in this paper, but in principle it can be replaced by any number greater than two.) On each subinterval a uniform mesh is constructed using $N/2$ mesh points in both $[0, \tau_2]$ and $[\tau_2, 1]$. The points of this piecewise uniform fitted mesh $\Omega^N_{\tau_2}$ in y-direction are then defined by

$$y_j = \begin{cases} \frac{2j\tau_2}{N} & \text{for } 0 \leqslant j \leqslant N/2, \\ \tau_2 + \frac{2(1-\tau_2)(j-N/2)}{N} & \text{for } N/2 < j \leqslant N. \end{cases} \tag{5.4}$$

The piecewise uniform fitted mesh is now defined as the tensor product

$$\Omega^{N\times N}_{\tau_1,\tau_2} = \Omega^N_{\tau_1} \times \Omega^N_{\tau_2}. \tag{5.5}$$

Note that $\Omega^{N\times N}_{\tau_1,\tau_2}$ is a uniform mesh whenever ε or N are sufficiently large.

Computed values of E^N_ε and E^N for Problem 2 are given in Table 5 for various values of ε and N.

The comments for Table 3 apply equally to Table 5. The ε-uniform rate of convergence p is estimated as before using the double-mesh principle. The results are given in Table 6.

Table 5
Maximum nodal errors E^N_ε and E^N on piecewise uniform fitted meshes $\Omega^{N\times N}_{\tau_1,\tau_2}$ for Problem 2

ε	N				
	8	16	32	64	128
2^0	1.792E − 2	1.019E − 2	5.306E − 3	2.647E − 3	1.230E − 3
2^{-2}	3.259E − 2	1.649E − 2	8.526E − 3	4.068E − 3	1.765E − 3
2^{-4}	1.310E − 1	8.292E − 2	5.457E − 2	3.071E − 2	1.403E − 2
2^{-6}	1.814E − 1	1.200E − 1	8.118E − 2	4.920E − 2	2.469E − 2
2^{-8}	2.023E − 1	1.458E − 1	9.417E − 2	5.664E − 2	2.973E − 2
2^{-10}	2.121E − 1	1.589E − 1	1.012E − 1	6.203E − 2	3.240E − 2
2^{-12}	2.166E − 1	1.654E − 1	1.046E − 1	6.489E − 2	3.381E − 2
2^{-14}	2.188E − 1	1.686E − 1	1.063E − 1	6.633E − 2	3.455E − 2
2^{-16}	2.199E − 1	1.702E − 1	1.071E − 1	6.704E − 2	3.491E − 2
2^{-18}	2.204E − 1	1.710E − 1	1.075E − 1	6.741E − 2	3.509E − 2
2^{-20}	2.207E − 1	1.714E − 1	1.078E − 1	6.763E − 2	3.519E − 2
2^{-22}	2.208E − 1	1.716E − 1	1.079E − 1	6.773E − 2	3.523E − 2
2^{-24}	2.209E − 1	1.717E − 1	1.079E − 1	6.779E − 2	3.525E − 2
2^{-26}	2.209E − 1	1.718E − 1	1.079E − 1	6.781E − 2	3.527E − 2
2^{-28}	2.210E − 1	1.718E − 1	1.079E − 1	6.783E − 2	3.527E − 2
2^{-30}	2.210E − 1	1.718E − 1	1.080E − 1	6.783E − 2	3.527E − 2
2^{-32}	**2.210E − 1**	**1.718E − 1**	**1.080E − 1**	**6.784E − 2**	**3.528E − 2**
E^N	0.2210	0.1780	0.1080	0.0678	0.0353

Table 6
Computed rates of convergence p using piecewise uniform fitted meshes $\Omega^{N\times N}_{\tau_1,\tau_2}$ for Problem 2

ε	N			
	8	16	32	64
2^{0}	0.814	0.942	1.003	1.105
2^{-2}	0.982	0.952	1.067	1.204
2^{-4}	0.660	0.604	0.829	1.130
2^{-6}	0.595	0.565	0.722	0.955
2^{-8}	0.473	0.631	0.733	0.930
2^{-10}	0.416	0.650	0.707	0.937
2^{-12}	0.389	0.660	0.690	0.940
2^{-14}	0.376	0.665	0.681	0.941
2^{-16}	0.370	0.668	0.677	0.941
.	.	.	.	.
.	.	.	.	.
.	.	.	.	.
2^{-32}	0.363	0.670	0.671	0.943

Again, these computed rates of ε-uniform convergence are consistent with the theoretical rate stated in the theorem in Appendix A. Note that the rates of convergence are increasing as N increases. They suggest that for Problem 2 the ε-uniform rate of convergence of this method is approaching $p = 1$.

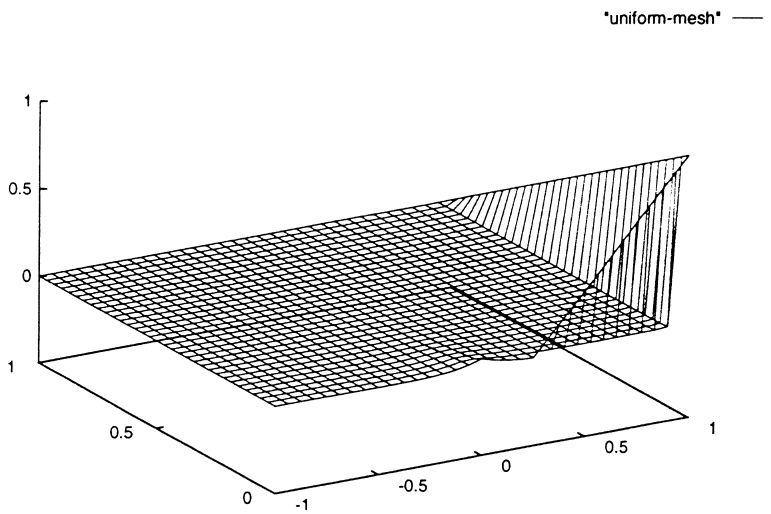

Fig. 7. Surface plot of the numerical solution of Problem 2 for $\varepsilon = 2^{-10}$ on the uniform mesh $\Omega^{32\times 32}$.

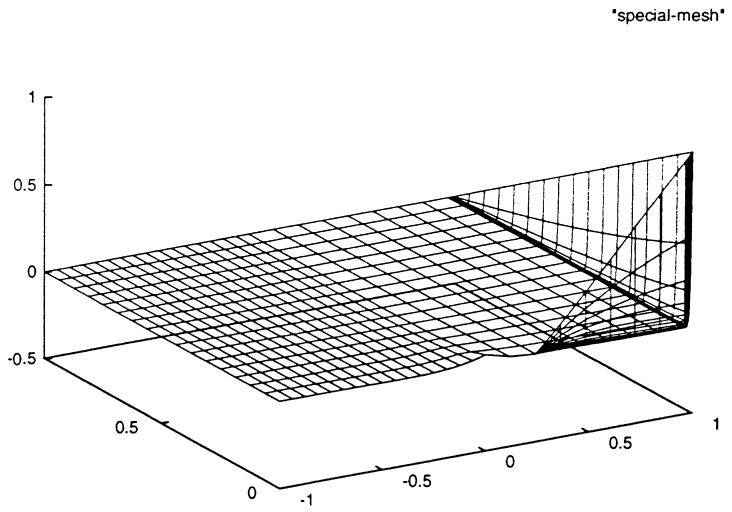

Fig. 8. Surface plot of the numerical solution of Problem 2 for $\varepsilon = 2^{-10}$ on the fitted mesh $\Omega^{32\times32}_{\tau_1,\tau_2}$.

The numerical solutions of Problem 2 for $\varepsilon = 2^{-10}$ on, respectively the uniform mesh $\Omega^{32\times32}$ and the fitted mesh $\Omega^{32\times32}_{\tau_1,\tau_2}$ are shown in Figs. 7 and 8.

Another view of the situation is obtained by comparing the contour plots of the numerical solution of Problem 2 for $\varepsilon = 2^{-10}$ on the uniform mesh $\Omega^{32\times32}$ in Fig. 9 and on the fine fitted mesh $\Omega^{256\times256}_{\tau_1,\tau_2}$ in Fig. 10.

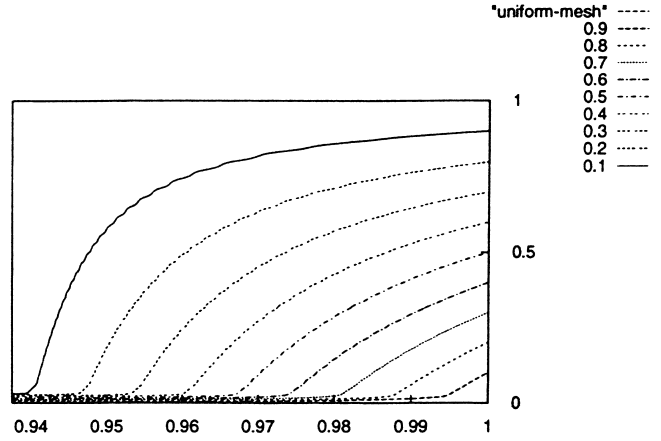

Fig. 9. Contour plot of the numerical solution of Problem 2 for $\varepsilon = 2^{-10}$ on the uniform mesh $\Omega^{32\times32}$ in a neighbourhood of the edge $x = 1$.

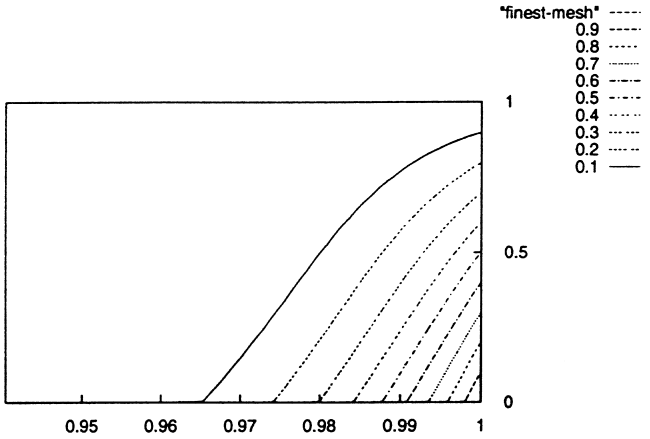

Fig. 10. Contour plot of the numerical solution of Problem 2 for $\varepsilon = 2^{-10}$ on the fine fitted mesh $\Omega^{256\times256}_{\tau_1,\tau_2}$ in a neighbourhood of the edge $x = 1$.

6. Additional computational experiments

Having established computationally that numerical methods based on appropriately fitted piecewise uniform meshes are ε-uniform, we look again at the numerical solutions of Problem 1 computed on uniform meshes, but now we estimate the error by using the ε-uniform method on the finest available piecewise uniform fitted mesh Ω^{512}_{τ} to approximate the exact solution of Problem 1. This approximation of the exact solution is then interpolated to the required uniform mesh, and the result is used to compute a new approximation to the error on this uniform mesh. The resulting computed errors are expected to be better approximations of the true error than those presented in Table 1. The results of this procedure are given in Table 7. Here it is seen more clearly than in Table 1 that the method is not ε-uniform. The remaining numerical experiments are designed to show that in order to obtain an ε-uniform method for Problem 2, it is essential to fit the mesh to all of the boundary layers rather than to just a subset of them.

In the first experiment Problem 2 is solved using piecewise uniform fitted meshes in the x-direction and uniform meshes in the y-direction. In the second experiment the converse is the case. Thus, in the first case the mesh is fitted only to the parabolic boundary layer, while in the second case it is fitted only to the regular boundary layer. The results are presented in Tables 8 and 9, respectively.

In these tables, the approximate nodal errors on a uniform mesh are estimated by the same procedure as was used for Table 7. We see clearly from Table 8, where the meshes are fitted only to the parabolic boundary layer, that

Table 7
Improved estimates of the maximum nodal errors E_{ε}^{N} and E^{N} on uniform meshes $\Omega^{N\times N}$ for Problem 1

ε	N					
	8	16	32	64	128	256
2^{0}	4.899E − 2	2.893E − 2	1.482E − 2	7.021E − 3	3.018E − 3	1.015E − 3
2^{-2}	3.279E − 2	2.775E − 2	1.561E − 2	7.481E − 3	3.177E − 3	1.060E − 3
2^{-4}	**6.486E − 2**	3.300E − 2	1.797E − 2	8.765E − 3	3.857E − 3	1.304E − 3
2^{-6}	5.480E − 2	**6.474E − 2**	3.129E − 2	1.611E − 2	7.218E − 3	2.473E − 3
2^{-8}	1.627E − 2	5.303E − 2	**6.139E − 2**	2.842E − 2	1.401E − 2	5.427E − 3
2^{-10}	1.193E − 2	1.566E − 2	5.227E − 2	**5.980E − 2**	2.764E − 2	1.375E − 2
2^{-12}	1.401E − 2	1.439E − 2	1.545E − 2	5.187E − 2	**5.894E − 2**	2.725E − 2
2^{-14}	1.458E − 2	1.607E − 2	1.057E − 2	1.536E − 2	5.166E − 2	**5.851E − 2**
2^{-16}	1.472E − 2	1.652E − 2	1.153E − 2	6.093E − 3	1.532E − 2	5.156E − 2
.	.	.	.	.	.	.
.	.	.	.	.	.	.
.	.	.	.	.	.	.
2^{-32}	1.477E − 2	1.668E − 2	1.188E − 2	6.745E − 3	3.286E − 3	1.229E − 3
E^{N}	0.0649	0.0647	0.0614	0.0598	0.0589	0.0585

Table 8
Maximum nodal errors E_{ε}^{N} and E^{N} on meshes $\Omega_{\tau_1}^{N\times N}$ fitted only to the parabolic boundary layer for Problem 2

ε	N					
	8	16	32	64	128	256
2^{0}	1.792E − 2	1.019E − 2	5.306E − 3	2.647E − 3	1.230E − 3	4.332E − 4
2^{-2}	3.259E − 2	1.649E − 2	8.526E − 3	4.068E − 3	1.765E − 3	5.924E − 4
2^{-4}	**1.448E − 1**	1.019E − 1	5.743E − 2	3.071E − 2	1.403E − 2	4.845E − 3
2^{-6}	1.095E − 1	**1.220E − 1**	**1.520E − 1**	**1.315E − 1**	7.243E − 2	3.745E − 2
2^{-8}	7.531E − 2	6.340E − 2	7.194E − 2	1.085E − 1	**1.585E − 1**	**1.509E − 1**
2^{-10}	6.478E − 2	4.890E − 2	3.779E − 2	3.906E − 2	5.946E − 2	1.068E − 1
2^{-12}	6.153E − 2	4.494E − 2	2.890E − 2	2.002E − 2	1.973E − 2	3.043E − 2
2^{-14}	6.046E − 2	4.411E − 2	2.659E − 2	1.563E − 2	9.830E − 3	9.079E − 3
2^{-16}	6.006E − 2	4.406E − 2	2.632E − 2	1.514E − 3	7.416E − 3	3.930E − 3
.	.	.	.	.	.	.
.	.	.	.	.	.	.
.	.	.	.	.	.	.
2^{-32}	5.977E − 2	4.402E − 2	2.630E − 2	1.513E − 2	7.323E − 3	2.775E − 3
E^{N}	0.1448	0.1220	0.1520	0.1315	0.1585	0.1509

Table 9
Maximum nodal errors E_{ε}^{N} and E^{N} on meshes $\Omega_{\tau_2}^{N\times N}$ fitted only to the regular boundary layer for Problem 2

ε	N					
	8	16	32	64	128	256
2^{0}	1.792E − 2	1.019E − 2	5.306E − 3	2.647E − 3	1.230E − 3	4.332E − 4
2^{-2}	3.259E − 2	1.649E − 2	8.526E − 3	4.068E − 3	1.765E − 3	5.924E − 4
2^{-4}	1.310E − 1	8.292E − 2	5.457E − 2	3.071E − 2	1.403E − 2	4.845E − 3
2^{-6}	**1.615E − 1**	1.384E − 1	8.555E − 2	4.920E − 2	2.469E − 2	9.255E − 3
2^{-8}	1.369E − 1	**1.534E − 1**	1.191E − 1	6.624E − 2	3.307E − 2	1.275E − 2
2^{-10}	1.271E − 1	1.313E − 1	**1.259E − 1**	9.287E − 2	4.560E − 2	1.894E − 2
2^{-12}	1.246E − 1	1.236E − 1	9.900E − 2	**9.523E − 2**	**7.132E − 2**	3.078E − 2
2^{-14}	1.239E − 1	1.217E − 1	9.058E − 2	6.924E − 2	6.944E − 2	**5.979E − 2**
2^{-16}	1.237E − 1	1.212E − 1	8.910E − 2	6.241E − 2	4.253E − 2	5.454E − 2
.	.	.	.	.	.	.
.	.	.	.	.	.	.
.	.	.	.	.	.	.
2^{-32}	1.237E − 1	1.210E − 1	8.861E − 2	6.009E − 2	3.216E − 2	1.254E − 2
E^{N}	0.1615	0.1534	0.1259	0.0952	0.0713	0.0598

the method is not ε-uniform, since the maximum error E^{256} is bigger than the maximum errors E^{8} and E^{16}. This shows that the additional computational effort due to the finer mesh is useless, because with more points we have a less accurate solution. This behaviour indicates that the method is not a satisfactory one.

The results in Table 9 are for meshes fitted only to the regular boundary layer. Since the errors E^N decrease only slowly with increasing N it is clear that the method is not ε-uniform.

7. Conclusions

It was shown from the numerical solutions of two particular problems that a standard numerical method, consisting of an upwind finite difference operator on a uniform mesh, gives inaccurate solutions to singularly perturbed linear convection–diffusion problems for heat transfer in a fluid with an assumed flow field in the neighbourhood of a 180° bend in a channel, when a parabolic boundary layer is present, and also when both parabolic and regular layers are present. Numerical computations were also presented which confirm the known theoretical result that ε-uniform methods can be constructed for these problems using upwind finite difference operators on piecewise uniform fitted meshes. In addition, further numerical experiments demonstrated that for such ε-uniform numerical methods it is necessary to fit the meshes to all of the boundary layers that are present.

Acknowledgements

The first author was supported by CICYT Project No. AMB 94-0396. The research of the fourth author was supported in part by the Russian Foundation for Basic Research under grant No. 98-01-00362.

Appendix A. Statement of a theoretical result for a class of problems

The main theoretical result concerning numerical methods, consisting of upwind finite difference operators on appropriately fitted piecewise uniform meshes, for solving a class of problems similar to (2.1a)–(2.1g), is contained in the following theorem. It states that these methods are ε-uniform, in the sense that the error bound and the rate of convergence are independent of the singular perturbation parameter ε. In order to state this theoretical result, it is

necessary to restrict the class of problems so that, in a neighbourhood of the corner $(1,1)$, the velocity field is of the form

$$\vec{u} = (2a_1(1-x^2), -2a_2(1-y^2)),$$

where a_1, a_2 are positive constants. For such problems the following theorem can be proved using the analytical techniques described in [13,14].

Theorem. *Let θ be the solution of the problem* (2.1a)–(2.1g) *or* (2.1a)–(2.1e) *and* (2.1h), *and let θ^N be the numerical approximation of θ computed using an upwind finite difference operator on the appropriate piecewise uniform fitted mesh. Then the following pointwise error estimate holds*:

$$\sup_{0<\varepsilon\leqslant 1} \max_{i,j} \mid \theta^N_{i,j} - \theta(x_i, y_j) \mid \leqslant C(N^{-1}\ln N)^{1/7},$$

where C is a constant independent of N and ε.

Note that Problems 1 and 2 considered in this paper do not satisfy the above condition on $\vec{u}$ near the corner point $(1,1)$. However, it is expected that this theorem can be extended to such problems, although this has not yet been proved rigorously.

References

[1] G.I. Shishkin, Discrete approximation of singularly perturbed elliptic and parabolic equations, Russian Academy of Sciences, Ural Section, Ekaterinburg, 1992 (in Russian).
[2] G.I. Shishkin, Difference scheme for singularly perturbed parabolic equation with discontinuous boundary condition, USSR Comput. Maths. Math. Phys. 28 (1988) 1649–1662 (in Russian).
[3] J.J.H. Miller, E. Mullarkey, E. O'Riordan, G.I. Shishkin, A simple recipe for uniformly convergent finite difference schemes for singularly perturbed problems, C.R. Acad. Sci. Paris 312 (1991) 643–648 (Serie I).
[4] C. Clavero, J.J.H. Miller, E. O'Riordan, G.I. Shishkin, An accurate numerical solution of a two dimensional heat transfer problem with a parabolic boundary layer, J. Comput. Math. 16 (1998) 27–39.
[5] J.J.H. Miller, E. O'Riordan, G.I. Shishkin, Fitted Numerical Methods for Singular Perturbation Problems, World Scientific, Singapore, 1996, xiv, p. 166.
[6] C.P. Thompson, N.S. Wilkes, Experiments with higher-order finite difference formulae, AERE-R10493, UK Atomic Energy Authority, Harwell, 1982.
[7] A.G. Hutton, The numerical representation of convection, IAHR Working Group Meeting, 1981.
[8] B. Scotney, Numerical experiments and error analysis for Petrov–Galerkin methods, Numer. Anal. Report, 11/82, University of Reading, 1982.
[9] R.M. Smith, A.G. Hutton, The numerical treatment of advection: a performance comparison of current methods, Numer. Heat Transfer 5 (1982) 439–461.
[10] K.W. Morton, Numerical Solution of Convection–Diffusion Problems, Chapman & Hall, London, 1995.

[11] A.F. Hegarty, J.J.H. Miller, E. O'Riordan, G.I. Shishkin, Special meshes for finite difference approximations to an advection–diffusion equation with parabolic layers, J. Comp. Phys. 117 (1995) 47–54.
[12] G. Guiding, On the solution of non-symmetric linear systems by the preconditioned conjugate gradient square method, INCA preprint No. 7, Dublin, 1987.
[13] G.I. Shishkin, Approximation of solutions of singularly perturbed boundary value problems with a corner layer, USSR Comput. Maths. Math. Phys. 27 (1987) 54–63.
[14] G.I. Shishkin, Numerical solution of elliptic equations with a small parameter at the highest order derivatives, Numer. Meth. Mech. Continuous Media 10 (1979) 107–124 (in Russian).